Development of bifacial n-type solar cells at Fraunhofer ISE: Status and perspectives

Fab & Facilities

Materials

Cell Processing

Thin Film

PV Modules

Power Generation

Market Watch

Sebastian Mack, **Elmar Lohmüller**, **Philip Rothhardt**, **Sebastian Meier**, **Sabrina Werner**, **Andreas Wolf**, **Florian Clement** & **Daniel Biro,** Fraunhofer Institute for Solar Energy Systems (ISE), Freiburg, Germany

ABSTRACT

This paper reports on the status of large-area, 156mm, bifacial, n-type passivated emitter and rear totally diffused (n-PERT) solar cells, which feature full-area homogeneous doped regions on the front and rear sides. The fabrication process includes either two separate gas-phase diffusion processes with sacrificial diffusion barrier layers, or a sophisticated co-diffusion approach, in which a deposited stack of borosilicate glass (BSG) and silicon oxide acts as a dopant source during back-surface field (BSF) formation in a tube furnace. Thus, the co-diffusion approach reduces the number of required high-temperature processes to one, which significantly streamlines the process sequence. It is shown that by implementing two deposition phases during the BSF diffusion process, it is possible to separately control both the depth and the surface concentration of the BSF. The use of a tailored BSG source allows low recombination and specific contact resistance values on both the front and rear sides, resulting in peak conversion efficiencies of 19.9%. A discussion on the recombination at the emitter–metal interface completes the paper, and several paths to driving the conversion efficiency towards 22% are outlined.

Introduction

During the last few years, n-type wafers and solar cells have been receiving more attention. The inherent advantages of n-type doped Czochralski-grown silicon (Cz-Si) wafers over p-type Cz-Si wafers are the absence of light-induced degradation (LID) [1], a reduced sensitivity against metal contaminations [2] – in particular iron – and a longer minority-carrier lifetime. The price of n-type Cz-Si wafers, however, is currently about 16% higher than that of p-type Cz-Si wafers [3], but this gap could become smaller in the future.

Compared with solar cells made from p-type silicon wafers, where the aluminium back-surface field (Al-BSF) cell and the passivated emitter and rear cell (PERC) are by far the two most dominant architectures, there are more concepts under investigation for cells made from n-type silicon. Both heterojunction with intrinsic thin layer (HIT) [4] and back-contact back-junction (BC-BJ) [5,6] solar cells are known for their high conversion efficiencies. Other promising cell concepts include rear-emitter structures, formed by either diffusion [7–10] or alloying a screen-printed aluminium layer [11,12], and the passivated emitter and rear locally diffused (PERL) [13] or passivated emitter and rear totally diffused (PERT) cells [14–16]. Also under consideration are n-type metal-wrap-through (n-MWT) solar cells [17,18].

Some of the above-mentioned architectures feature a rear surface that is only partially metallized, which makes them potentially interesting for bifacial applications. With adaptations of the module layout, an additional energy yield of the order of 20% has been reported [19,20], at almost no additional cost; this is certainly one of the reasons why the ITRPV roadmap forecasts a market share increase for n-type solar cells from 5% in 2013 to almost 40% in 2024 [21]. In addition, it is worth mentioning that bifacial solar cells are developed not solely for n-type substrates, but also for p-type wafers [22,23]. For an overview of bifacial systems and recent progress in this field, see Kopecek et al. [24].

This paper reports on the status of bifacial n-PERT solar cells and R&D activities at Fraunhofer ISE. After a presentation of a fabrication process with sequential diffusion processes, this process is simplified by an implementation of the compact co-diffusion approach, in which a deposited borosilicate glass acts as a dopant source for emitter formation during a gas-phase diffusion process for back-surface field formation. The properties of the diffusion process as well as of the doping profiles produced are characterized, and saturation current densities and specific contact resistance values are reported. One dedicated section addresses the recombination at the emitter–metal interface and describes ways to reduce that particular contribution to the overall recombination.

Sequential diffusion approach

In the reference process for the fabrication of bifacial H-pattern cells, 156mm n-type Cz-Si wafers with a base resistivity between 3 and 6Ωcm are used. After random pyramid formation in alkaline solution, the boron emitter and the phosphorus BSF are formed by two sequential tube-furnace diffusion processes using boron tribromide (BBr_3) and phosphorus oxychloride ($POCl_3$) as dopant sources. Obviously one has to ensure selective doping of each side during this sequence, and this is accomplished by the use of sacrificial dielectric diffusion barrier layers, applied prior to each diffusion.

As BBr_3 diffusion takes place at temperatures considerably higher than those for $POCl_3$ diffusion, it was decided to perform the BBr_3 diffusion first, in order to minimize profile changes during the second high-temperature step [25]. A clear advantage of this approach is the possibility of optimizing each diffusion process separately, at least to a large extent. A disadvantage is the use of two high-temperature processes; this could possibly affect the minority-carrier lifetime in the bulk, as well as putting some cost pressure on the process sequence.

After the second diffusion process and glass removal, a dielectric stack of aluminium oxide (Al_2O_3) and silicon nitride (SiN_x) is deposited by plasma-
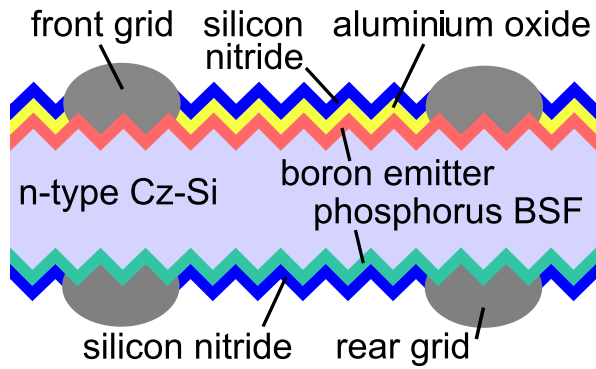
Figure 1. Schematic cross section of a bifacial n-PERT solar cell with an H-pattern grid on both the front and back sides.
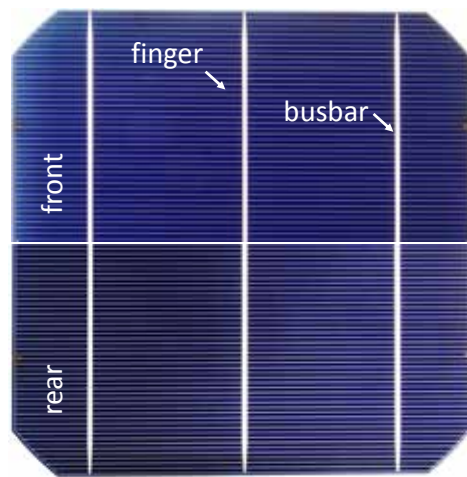
Figure 2. Photographs of the front and back sides of a bifacial n-type solar cell with an H-pattern grid. The cell layout is suited to bifacial applications, for example in glass–glass modules or in modules with transparent backsheets.

enhanced chemical vapour deposition (PECVD) on the front side, whereas on the rear side a single PECVD-SiN$_x$ layer is deposited. Front-contact formation is realized by screen printing a AgAl paste, whereas a Ag paste is used on the rear side. After contact firing, laser edge isolation ensures the electrical insulation between the front and rear sides.

Fig. 1 shows a schematic cross section of a bifacial n-PERT solar cell in a standard H-pattern layout; the top and bottom views are illustrated in the photograph in Fig. 2. Conversion efficiencies of 19.7%, measured in a cell tester on a white and non-conductive foil, have been achieved using the sequential diffusion approach.

Simplified process sequence using co-diffusion

As discussed above, in the fabrication of the investigated H-pattern bifacial solar cells it is necessary to provide doping profiles of different polarities on the front and rear sides of the device. Although this can be achieved, for example, by applying diffusion barriers and two subsequent gas-phase diffusion processes, it would be more convenient to restrict the dopant formation to one side of the sample and perform only one high-temperature step.

"The co-diffusion approach investigated at Fraunhofer ISE permits a largely independent adjustment of boron and phosphorus doping profiles."

Figure 3. (a) Process flow for the fabrication of bifacial n-PERT solar cells. After BSG/SiO$_x$ dielectric layer stack deposition, co-diffusion takes place in a POCl$_3$ diffusion process. (b) Schematic cross section of the samples before co-diffusion in a POCl$_3$ atmosphere.

Recently, more attention has especially been given to ion implantation [26–28] and diffusion from deposited doped glasses [29–34]. Both require a subsequent high-temperature step for respectively dopant activation and drive-in. One approach is to implant or cap both sides of the wafer and perform one thermal treatment in an inert gas or in an atmosphere with a low oxygen content [35]. Both co-annealing and co-diffusion significantly streamline the process sequence, but the degree of freedom for independent control of the doping profiles is reduced, as the dose for each dopant type can only be chosen in advance and cannot be adjusted during the thermal process. The ups and downs of both process sequences have already been nicely summarized by Lim et al. [36]. The co-diffusion approach investigated at Fraunhofer ISE, which combines the diffusion from a deposited glass with that from a gas-phase diffusion process, overcomes the above-described limitation, since it permits a largely independent adjustment of boron and phosphorus doping profiles.

For the fabrication of co-diffused bifacial large-area n-PERT solar cells, denoted CoBiN (co-diffused bifacial n-type) [32], n-type Cz-Si wafers with an edge length of 156mm and a base resistivity of $3\Omega cm$ are used; the process flow is depicted in Fig. 3(a). A layer stack of borosilicate glass (BSG) and silicon oxide (SiO_x), deposited by atmospheric pressure chemical vapour deposition (APCVD) (in cooperation with SCHMID Group), is used as a dopant source for emitter formation during BSF formation in a $POCl_3$ atmosphere (see Fig. 3 (b)), in the standard phosphorus tube-furnace diffusion system that is widely used today in the PV industry. Other groups have also successfully applied the boron source by alternative methods, such as PECVD [29,30,33], spin-on [37] or inkjet printing [35]. Recently, Mitsubishi reported the use of an APCVD-BSG layer for emitter formation in bifacial n-PERT solar cells as well, yielding conversion efficiencies above 21% [31].

After front-surface passivation with an Al_2O_3 layer in an inline atomic layer deposition (ALD) tool, the SiN_x anti-reflection coating and the silicon oxynitride (SiO_xN_y)/SiN_z

rear-passivation stack are deposited by PECVD. In this experiment, the front contact has been formed by dual printing (printing the busbars and fingers in different process steps), where Ag paste is applied for the floating busbar and AgAl paste for the fingers. Both the front AgAl fingers and the subsequently printed rear Ag fingers are formed by print-on-print (double-printing) technology, using the same grid and paste for each printing step twice. Contact firing and laser edge isolation complete the process sequence.

Solar cells fabricated with the CoBiN process sequence have demonstrated conversion efficiencies of up to 19.9% (see Table 1) on a reflecting, conductive chuck (calibrated measurements at Fraunhofer ISE CalLab PVCells); these values are similar to those reported by other authors [30,36,38]. Measurements taken on a black, non-conductive chuck yield a conversion efficiency of only 19.5%, which highlights the impact of the measurement conditions on the conversion efficiency in the case of bifacial cells.

Böscke et al. [16] have reported that measurements on a non-reflective,

Measurement chuck	V_{oc} [mV]	J_{sc} [mA/cm^2]	FF [%]	η [%]	R_p [kΩcm^2]
Black, non-conductive	647	38.3	78.7	19.5	19
Golden, conductive	648	38.8	79.0	19.9	19
Combined	648	38.8	78.7	19.8	19

Table 1. *I–V* data of large-area bifacial n-type co-diffused CoBiN solar cells, extracted from calibrated measurements at Fraunhofer ISE CalLab PVCells. The parallel resistance R_p is determined from a measurement in an industrial cell tester.
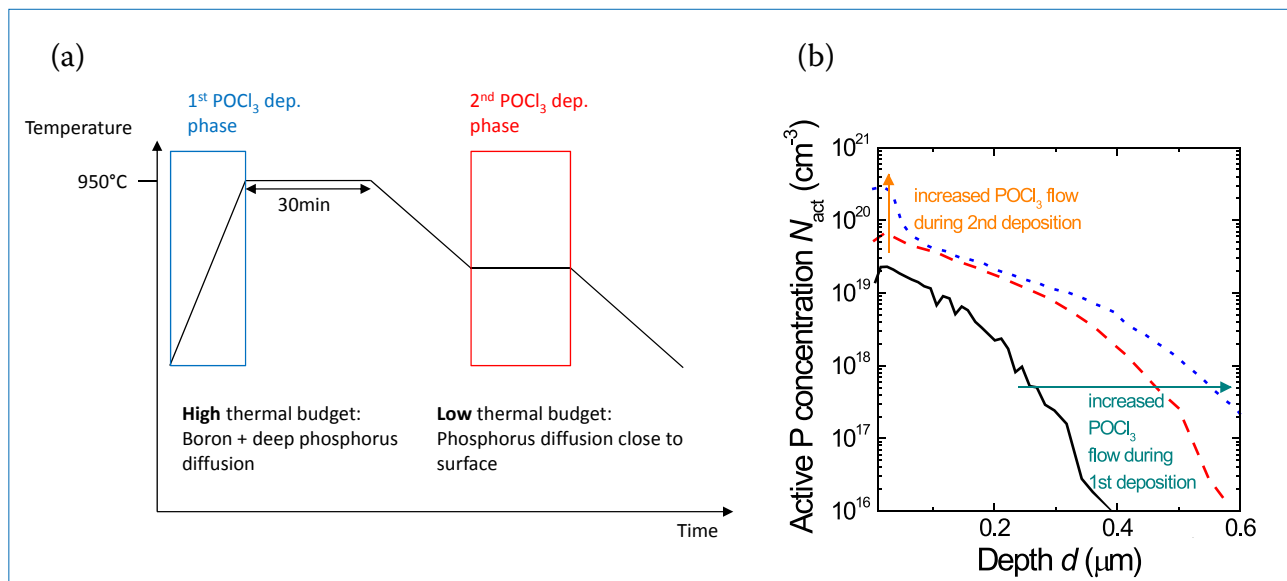
Figure 4. (a) Temperature–time profile of the $POCl_3$ diffusion process, highlighting two deposition phases, which allows independent control of the depth and surface concentration of the phosphorus doping profile. Drive-in of the boron emitter out of the APCVD-BSG/SiO$_x$ stack takes place during the first deposition step at 950℃. **(b)** The resulting phosphorus profiles, measured by electrochemical capacitance voltage (ECV) profiling on alkaline saw-damage-etched surfaces.

non-conductive chuck show a decrease in both J_{sc} and FF compared with a reflective, conductive chuck. Since no norm yet exists relating to how bifacial cells or modules should be measured, the calculation of a combined efficiency has been proposed, which includes V_{oc} and J_{sc} from the measurement on the reflective chuck and FF from the measurement on the non-conductive chuck. This results in a combined efficiency of 19.8% for Fraunhofer ISE cells.

When measuring bifacial n-PERT solar cells, it is important to look not only at the forward current but also at the reverse bias stability; as several authors have shown, this might be a bigger challenge for these cells than for p-type cells [15,28,39].

Layer and doping profile properties

In the POCl$_3$ co-diffusion process developed at Fraunhofer ISE, with a temperature–time profile depicted in Fig. 4(a), the use of different deposition phases makes it possible to separately control the depth and surface concentration of the BSF. The POCl$_3$ flow in the first deposition phase controls the depth of the phosphorus BSF; in addition, the temperature of 950°C allows the drive-in of the boron out of the pre-deposited BSG source.

> "The use of different deposition phases makes it possible to separately control the depth and surface concentration of the BSF."

Changes in the POCl$_3$ bubbler gas flow during the second deposition phase, towards the end of the process, affect the surface concentration of the doping profile (see Fig. 4(b)); the profile can be tailored to achieve a low specific contact resistance between the phosphorus BSF and the screen-printed Ag contacts. Thus, an independent manipulation of BSF depth and surface concentration is possible in a single process, while the BSG composition and thermal budget of the process control the boron doping profile.

Fig. 5 shows the specific contact resistance ρ_c and dark saturation current density $J_{0,BSF}$ of phosphorus BSFs for variations in the POCl$_3$ gas flow in the second deposition phase. The contacts have been formed by the screen printing of Ag paste followed by contact firing. As expected from the diffusion profile, transfer length method (TLM)

measurements reveal low ρ_c values, between 2mΩcm^2 and 4mΩcm^2, for a wide range of POCl$_3$ flow rates, when a second deposition phase is introduced.

The $J_{0,BSF}$ values shown in Fig. 5 were extracted in high-level injection on symmetric n-type Cz-Si samples with alkaline-textured surfaces after passivation by either a PECVD-SiN$_x$ layer or a PECVD-SiO$_x$N$_y$/SiN$_z$ stack and contact firing. For a flow rate of 200sccm, which was the lowest tested flow rate in this experiment, $J_{0,BSF}$ amounts to 125fA/cm^2 for a SiO$_x$N$_y$/SiN$_z$ passivation stack. This flow rate (200sccm) is also used for BSF formation in Fraunhofer ISE solar cells. Fraunhofer ISE's POCl$_3$ process was recently enhanced to allow $J_{0,BSF}$ values below 100fA/cm^2, and the process time was shortened, while improving at the same time the sheet resistance homogeneity over the wafer.

The question arises as to whether the deposited BSG/SiO$_x$ stack is

really impervious to phosphorus and completely blocks the phosphorus diffusion from the gas phase. To address this point a secondary ion mass spectrometry (SIMS) was performed on shiny-etched wafers after layer deposition and POCl$_3$ diffusion; measurements of the respective atomic concentration in the dielectric layers as well as in the silicon wafer were taken. The results are shown in Fig. 6, with a proposed layer arrangement indicated above the graph.

At the surface of the samples, the POCl$_3$ from the atmosphere reacts with the bare SiO$_x$ layer to form a phosphorus silicon glass (PSG). The high concentration gradient might lead to some phosphorus diffusion through the SiO$_x$ and BSG layer, as highlighted by a P concentration of around 10^{17}cm^{-3} in the silicon wafer itself; however, that concentration is a few orders of magnitude below that of the boron concentration. Interestingly,
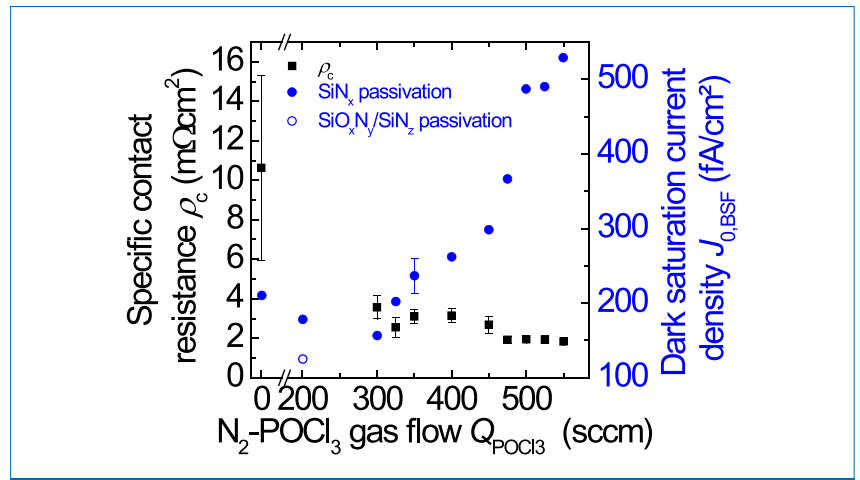
Figure 5. Specific contact resistance ρ_c and dark saturation current density $J_{0,BSF}$ of phosphorus-diffused BSFs for different POCl$_3$ gas flows. A PECVD-SiN$_x$ layer or a SiO$_x$N$_y$/SiN$_z$ stack was used for surface passivation.
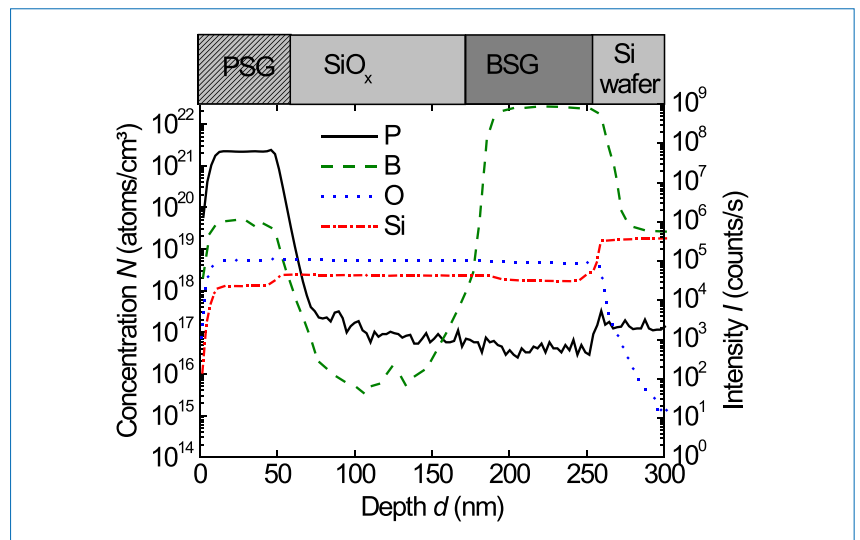
Figure 6. SIMS measurements of BSG/SiO$_x$ layer stack after POCl$_3$ diffusion. The proposed sample structure is shown above the graph.

the high boron concentration gradient leads to a boron diffusion through the SiO_x layer into the PSG, resulting in concentrations above $10^{19}cm^{-3}$, whereas in the SiO_x layer itself a very low boron concentration of $10^{16}cm^{-3}$ is measured.

From the results it is concluded that, even if there might be some diffusion of phosphorus through the BSG/SiO_x stack, it will not negatively impact the boron diffusion profile; this is confirmed by identical boron doping profiles measured for diffusion processes with and without $POCl_3$ in the process atmosphere. Similar results are expected in the solar cell, where the dielectric stack is deposited on alkaline-textured surfaces.

The resulting boron emitter profiles themselves are characterized by a sheet resistance of 77Ω/sq. and $J_{0e} = 57fA/cm^2$, measured in high-level injection on symmetrically textured n-type Cz-Si samples after passivation by an Al_2O_3/SiN_x stack and activation of the passivation layers in a firing furnace. After a screen printing of AgAl paste and contact firing, TLM measurements yield $\rho_c = 2m\Omega cm^2$, which is similar in value to that of the diffused boron profiles from the gas phase.

Boron emitter metallization

Inherent in boron profiles that are suitable for screen-printed contacts using AgAl paste is a rather high recombination $J_{0e,met}$ at the semiconductor–metal interface. Values of $J_{0e,met}$ in the range 3500–4200fA/cm^2 have recently been reported [17,40], which might be the result of deep spike penetration of the AgAl paste into the wafer surface and emitter; these values are a couple of times higher than those seen for Ag pastes on the phosphorus BSF. Although the metallized area fraction A_{met} at the front of solar cells is only a few per cent, the J_0 contribution of the AgAl contacts is about two to four times higher than that of the passivated area J_{0e}. As a result, efforts to reduce A_{met} are being made.

One approach is dual printing of the AgAl front contact, where printing takes place in two separate steps and different pastes are used for the busbar and fingers. The implementation of floating Ag busbars in H-pattern cells thus reduces A_{met} of the AgAl paste from 5.8% to 3.4%, which in this case increases the open-circuit voltage V_{oc} by 7mV. However, the shaded-area fraction remains unchanged. Another approach is the integration of MWT structures, where moving the busbars from the front to the rear not only decreases A_{met} compared with contacting busbars, but also reduces shading.
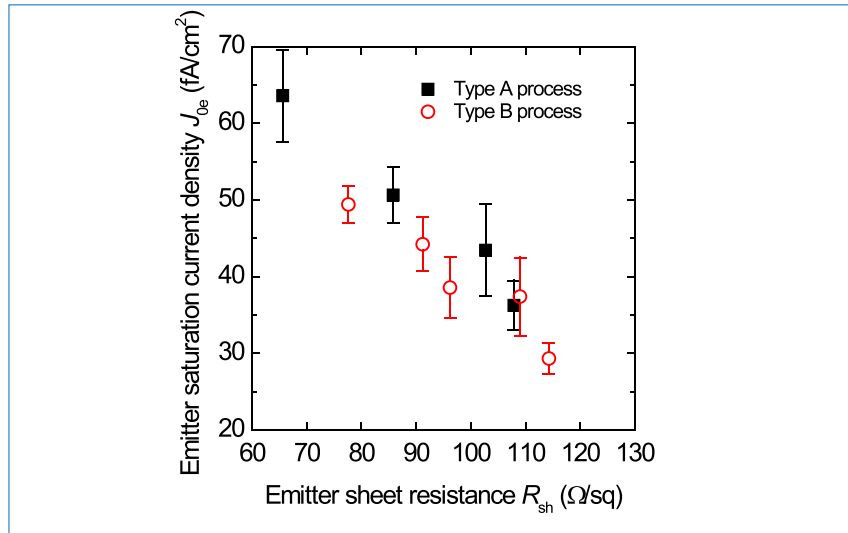
Figure 7. Emitter saturation current density J_{0e} plotted vs. the sheet resistance R_{sh} for symmetric, alkaline-textured, 10Ωcm, n-type Cz-Si wafers. The J_{0e} determination is performed in high-level injection after passivation with an Al_2O_3/SiN_x stack by PECVD and contact firing.

An alternative approach to reducing front-metallization-related recombination is an adaptation of the boron diffusion process. Edler et al. [40] have shown that increasing the profile depth while keeping the surface concentration unchanged is effective in reducing $J_{0e,met}$. This indicates a possible window for selective boron emitters, which might, however, be made obsolete by improvements in metallization pastes, as seen in the case of phosphorus emitters in the past. Adaptations of Fraunhofer ISE's BBr_3 diffusion process have made it possible to decrease J_{0e} by increasing the depth and reducing the surface concentration of the emitter profile to values down to 30fA/cm^2 on alkaline-textured surfaces (see Fig. 7). Here, the surfaces are passivated by a fired Al_2O_3/SiN_x layer stack, with 'Type A' and 'Type B' referring to different processes. Initial TLM measurements reveal specific contact resistance values in the low mΩcm^2 range for all 'Type A' processes using a commercially available AgAl paste; however, the $J_{0e,met}$ determination is still pending.

Another promising option for reducing $J_{0e,met}$ might also be the replacement of screen-printed contacts by plated Ni/Cu contacts, if process maturity is ensured; this could very likely be combined with an adaptation of the emitter profile as indicated above.

Conclusions

For the fabrication of bifacial n-PERT front-junction solar cells, a reference process has been established, which is based on two sequential diffusion processes and which allows conversion efficiencies of up to 19.7% in H-pattern cells, measured on a white, non-

conductive foil. It has been shown that the detrimental impact of high front-contact recombination can be reduced by the implementation of floating Ag busbars, which increases V_{oc} by 7mV.

The process sequence has been further greatly simplified by substituting a co-diffusion process for the two sequential diffusion processes. An APCVD process forms the BSG/SiO_x stack for emitter formation on the front side of the samples, followed by a drive-in during BSF formation in a $POCl_3$ atmosphere. The $POCl_3$ diffusion process contains two deposition phases; this allows independent manipulation (to a large extent) of both depth and surface concentration of the BSF. Bifacial solar cells with a conversion efficiency of up to 19.9% have been fabricated with this CoBiN process. Further increases in conversion efficiency are expected in the near future through improvements to the $POCl_3$ diffusion process, adaptations of the BSG source and new metallization pastes.

The fact that $POCl_3$ diffusion furnaces are widely available and facilitate high throughput, as well as the similarities of the CoBiN process sequence to p-type PERC solar cell fabrication, reduces the barriers to industrial implementation.

"A TOPCon layer implementation could increase the conversion efficiency of bifacial n-PERT front-junction solar cells to over 22% in the near future."

Outlook

To address the high carrier recombination at the screen-printed AgAl emitter contact, it is planned to adapt Fraunhofer ISE's BSG source and $POCl_3$ diffusion process accordingly. Improved metallization pastes will be applied for the screen-printed contacts route, or, alternatively, fully plated contacts on both the front and the rear will be included. This will decrease not only $J_{0e,met}$ but also J_{0e} in the passivated regions and thus result in a higher open-circuit voltage. Simulations with Sentaurus Device indicate a conversion efficiency potential of over 22% for such cells.

Another option is to adapt the cell structure itself and include a polysilicon [41,42] or a TOPCon (tunnel oxide passivated contact) layer for a carrier-selective rear contact. With monofacial solar cells of size 2cm × 2cm with a planar rear side, the excellent passivation quality of the TOPCon layer has yielded open-circuit voltages of 715mV and conversion efficiencies greater than 24% [43]; a very good passivation quality on textured surfaces, however, has already also been demonstrated by Moldovan et al. [44], with a V_{oc} limit of 715mV. Since recombination in the BSF region is the second-highest loss factor after $J_{0e,met}$ in the CoBiN cell structure, a TOPCon layer implementation could increase the conversion efficiency of bifacial n-PERT front-junction solar cells to over 22% in the near future.

References

[1] Glunz, S.W. et al. 2001, "Minority carrier lifetime degradation in boron-doped Czochralski silicon", *J. Appl. Phys*, Vol. 90, pp. 2397–2404.

[2] Istratov, A.A., Hieslmair, H. & Weber, E.R. 1999, "Iron and its complexes in silicon", *Appl. Phys. A*, Vol. A69, pp. 13–44.

[3] PVInsights 2015, Solar Wafer Monthly Contract Price (9th Feb.) [http://pvinsights.com/].

[4] Masuko, K. et al. 2014, "Achievement of more than 25% conversion efficiency with crystalline silicon heterojunction solar cell", *IEEE J. Photovolt.*, Vol. 4, pp. 1433–1435.

[5] Franklin, E. et al. 2014, "Fabrication and characterization of a 24.4% efficient IBC cell", *Proc. 29th EU PVSEC*, Amsterdam, The Netherlands.

[6] Smith, D.D. et al. 2013, "SunPower's Maxeon Gen III solar cell: High efficiency and energy yield", *Proc. 39th IEEE PVSC*, Tampa, Florida, USA.

[7] Lim, B. et al. 2014, "n-PERT back junction solar cells: An option for the next industrial technology generation?", *Proc. 29th EU PVSEC*, Amsterdam, The Netherlands.

[8] Duerinckx, F. et al. 2014, "Quantifying internal optical losses for 21% n-Si rear junction cells", *Proc. 29th EU PVSEC*, Amsterdam, The Netherlands.

[9] Mertens, V. et al. 2013, "Large area n-type Cz double side contact back junction solar cell with 21.3% conversion efficiency", *Proc. 28th EU PVSEC*, Paris, France.

[10] Degans, H. 2015, "Imec demonstrates large area industrial crystalline silicon n-PERT solar cell with a record 22 percent efficiency", Press Release (Jan.) [http://www2.imec.be/be_en/press/imec-news/imec-22-percent-npert-solar-cell.html].

[11] Schmiga, C. et al. 2012, "Status and perspectives on n-type silicon solar cells with aluminium-alloyed rear emitter", *Proc. 27th EU PVSEC*, Frankfurt, Germany.

[12] Xi, X. et al. 2012, "High efficiency aluminum-rear-emitter n-type silicon solar cells with inline phosphorus diffusion process on the front surface", *Proc. 27th EU PVSEC*, Frankfurt, Germany.

[13] Steinhauser, B. et al. 2014, "Firing-stable PassDop passivation for screen printed n-type PERL solar cells based on a-SiN$_x$:P", *Solar Energy Mater. & Solar Cells*, Vol. 126, pp. 96–100.

[14] Tao, Y. et al. 2014, "20.7% efficient ion-implanted large area n-type front junction silicon solar cells with rear point contacts formed by laser opening and physical vapor deposition", *Progr. Photovolt.: Res. Appl.*, Vol. 22, pp. 1030–1039.

[15] Blévin, T. et al. 2014, "Development of industrial processes for the fabrication of high efficiency n-type PERT cells", *Solar Energy Mater. & Solar Cells*, Vol. 131, pp. 24–29.

[16] Böscke, T. et al. 2013, "Bifacial n-type cells with >20% front-side efficiency for industrial production", *IEEE J. Photovolt.*, Vol. 3, pp. 674–677.

[17] Lohmüller, E. et al. 2014, "The HIP-MWT+ solar cell concept on n-type silicon and metallization-induced voltage losses", *Proc. 29th EU PVSEC*, Amsterdam, The Netherlands.

[18] Guillevin, A. et al. 2014, "High efficiency n-type metal-wrap-through cells and modules using industrial processes", *Proc. 29th EU PVSEC*, Amsterdam, The Netherlands.

[19] Grunow, P. 2012, "Bifacial modules – Promises and challenges", bifipv-workshop, Konstanz, Germany.

[20] Van Aken, B.B. et al. 2014, "Relation between indoor flash testing and outdoor performance of bifacial modules", *Proc. 29th EU PVSEC*, Amsterdam, The Netherlands.

[21] SEMI PV Group Europe 2014, "International technology roadmap for photovoltaic (ITRPV): Results 2013", 5th edn (Mar.) [http://www.itrpv.net/Reports/Downloads/].

[22] Fertig, F. et al. 2014, "The BOSCO solar cell – A both sides collecting and contacted structure", *physica status solidi (RRL)*, Vol. 8, pp. 381–384.

[23] ERDM Solar/SCHMID Group 2014, "ERDM Solar and SCHMID Group announce the supply agreement for the world's first full GEMINUS bifacial turnkey cell and module manufacturing line with multi bus bar module technology", Press Release (Dec.) [http://www.schmid-group.com/en/press-%2B-news/press-releases/p180/erdm-solar-and-schmid-group-announce-the-supply-agreement-for-the-worlds-first-full-geminus-bifacial-turnkey-cell-and.html].

[24] Kopecek, R. et al. 2014, "Bifaciality: One small step for technology, one giant leap for kWh cost reduction", *Photovoltaics International*, 26th edn, pp. 32–45.

[25] Lohmüller, E. et al. 2013, "Depletion of boron-doped surfaces protected with barrier layers during $POCl_3$-diffusion", *Proc. 28th EU PVSEC*, Paris, France.

[26] Benick, J. et al. 2012, "Fully implanted n-type PERT solar cells", *Proc. 27th EU PVSEC*, Frankfurt, Germany.

[27] Kiefer, F. et al. 2014, "Influence of the boron emitter profile on V_{oc} and J_{sc} losses in fully ion implanted n-type PERT solar cells", *physica status solidi (a)*, DOI 10.1002/pssa.201431118, pp. 1–7.

[28] Böscke, T. et al. 2014, "Fully ion implanted and coactivated industrial n-type cells with 20.5% efficiency", *IEEE J. Photovolt.*, Vol. 4, pp. 48–51.

[29] Cabal, R. et al. 2009, "Investigation of the potential of boron doped oxide deposited by PECVD – Application to advanced solar cells fabrication processes", *Proc. 24th EU PVSEC*, Hamburg, Germany.

[30] Frey, A. et al. 2014, "N-type bi-facial solar cells with boron emitters from doped PECVD layers", *Proc. 29th EU PVSEC*, Amsterdam, The Netherlands.

[31] Nishimura, S. et al. 2014, "Over 21% efficiency n-type monocrystalline silicon photovoltaic cell with boron doped emitter", *Tech. Digest 6th WCPEC*, Kyoto, Japan.

[32] Rothhardt, P. et al. 2014, "Codiffused bifacial n-type solar cells (CoBiN)", *Energy Procedia*, Vol. 55, pp. 287–294.

[33] Wehmeier, N. et al. 2013, "Boron-doped silicon oxides as diffusion sources for simplified high-efficiency solar cell fabrication", *Proc. 28th EU PVSEC*, Paris, France.

[34] Rothhardt, P. et al. 2012, "Control of phosphorus doping profiles for co-diffusion processes", *Proc. 27th EU PVSEC*, Frankfurt, Germany.

[35] Keding, R. et al. 2014, "POCl₃-based co-diffusion process for n-type back-contact back-junction solar cells", *Proc. 29th EU PVSEC*, Amsterdam, The Netherlands.

[36] Lim, B. et al. 2014, "Simplifying the fabrication of n-PERT solar cells: Recent progress at ISFH", *Photovoltaics International*, 26th edn, pp. 46–54.

[37] Barth, S. et al. 2013, "Bifacial solar cells with highly efficient spin-on boron diffusion", *Proc. 28th EU PVSEC*, Paris, France.

[38] Cabal, R. et al. 2014, "20% PERT technology adapted to n-type mono-like silicon: Simplified process and narrowed cell efficiency distribution", *Proc. 29th EU PVSEC*, Amsterdam, The Netherlands.

[39] Lohmüller, E. et al. 2014, "Reverse bias behavior of diffused and screen-printed n-type Cz-Si solar cells", *IEEE J. Photovolt.*, Vol. 4, pp. 1483–1490.

[40] Edler, A. et al. 2014, "Metallization-induced recombination losses of bifacial silicon solar cells", *Progr. Photovolt.: Res. Appl.*, DOI: 10.1002/pip.2479.

[41] Römer, U. et al. 2014, "Ion-implanted poly-Si / c-Si junctions as a back-surface field in back-junction back-contacted solar cells", *Proc. 29th EU PVSEC*, Amsterdam, The Netherlands.

[42] Stradins, P. et al. 2014, "Passivated tunneling contacts to n-type wafer silicon and their implementation into high performance solar cells", *Tech. Digest 6th WCPEC*, Kyoto, Japan.

[43] Feldmann, F. et al. 2014, "Tunnel oxide passivated contacts as an alternative to partial rear contacts", *Solar Energy Mater. & Solar Cells*, Vol. 131, pp. 46–50.

[44] Moldovan, A. et al. 2014, "Simple cleaning and conditioning of silicon surfaces with UV/ozone surfaces", *Energy Procedia*, Vol. 55, pp. 834–844.

About the Authors

Sebastian Mack holds a diploma degree in physics from the University of Jena and a doctoral degree in physics from the University of Konstanz, Germany. For his doctoral thesis he investigated thermal oxidation processes for industrial high-efficiency PERC solar cells at Fraunhofer ISE. Sebastian is currently a postdoctoral researcher in the Thermal Processes / Passivated Solar Cells Group at Fraunhofer ISE, where his interests include high-temperature processing and process development for p- and n-type silicon solar cells.

Elmar Lohmüller studied physics at the University of Tübingen and at Nelson Mandela Metropolitan University, Port Elizabeth, South Africa. He received his diploma degree in 2010 and for his thesis worked at Fraunhofer ISE on the development of p-type MWT-PERC solar cells. Elmar is currently working on his dissertation, focusing on the development of n-type MWT solar cells.

Philip Rothhardt received a master's in physics from Humboldt University of Berlin, and a Ph.D., also in physics, in 2014 from the University of Freiburg, Germany. The work for his doctorate, carried out at Fraunhofer ISE, involved the development and characterization of co-diffusion processes for n-type solar cells.

Sebastian Meier studied physics at the University of Freiburg and at Pierre and Marie Curie University in Paris. In 2014 he received his diploma degree, the thesis work for which was carried out at Fraunhofer ISE on the development of bifacial n-type solar cells based on co-diffusion. He recently began working on his dissertation, focusing on the development of co-diffused bifacial n- and p-type solar cells.

Sabrina Werner studied physics at the University of Freiburg, Germany, receiving her diploma degree in 2011. Since then she has been working in the Photovoltaic Production Technology and Quality Assurance Division at Fraunhofer ISE. Her research interests include the improvement of high-temperature processes and passivated solar cells.

Andreas Wolf studied physics at the Technical University of Darmstadt and at the KTH Royal Institute of Technology in Stockholm. He received his Ph.D. from the Leibniz University of Hanover in 2007. Andreas is head of the Thermal Processes / Passivated Solar Cells Group at Fraunhofer ISE.

Florian Clement received his doctorate in 2009 from the University of Freiburg. He is currently head of the MWT Solar Cells and Printing Technology Group at Fraunhofer ISE, where his research interests include the development of highly efficient pilot-line-processed metal-wrap-through solar cells, as well as the development and evaluation of printing technologies.

Daniel Biro studied physics at the University of Karlsruhe, Germany, and at the University of Massachusetts Amherst, USA. He received his Ph.D. in the field of silicon solar cell diffusion technologies from the University of Freiburg in 2003. During 2004–2005 he coordinated the design and ramp-up of the production-oriented research platform PV-TEC and is currently head of the Thermal, PVD, and Printing Technology / Industrial Cell Structures Department at Fraunhofer ISE.

Enquiries

Fraunhofer Institute for Solar Energy Systems (ISE)

Heidenhofstr. 2
79110 Freiburg
Germany

Tel: +49 (0) 761 4588 0
Email: info@ise.fraunhofer.de

Website: www.ise.fraunhofer.de